Terahertz achromatic quarter-wave plate

Jean-Baptiste Masson, Guilhem Gallot

HAL Id: hal-00827921
https://polytechnique.hal.science/hal-00827921

Terahertz achromatic quarter-wave plate

Jean-Baptiste Masson and Guilhem Gallot

Laboratoire d'Optique et Biosciences, CNRS UMR 7645, INSERM U696, École Polytechnique,
91128 Palaiseau, France

Phase retarders usually present a strong frequency dependence. We discuss the design and characterization of a terahertz achromatic quarter-wave plate. This wave plate is made from six birefringent quartz plates precisely designed and stacked together. Phase retardation has been measured over the whole terahertz range by terahertz polarimetry. This achromatic wave plate demonstrates a huge frequency bandwidth ($\nu_{max}/\nu_{min} \approx 7$), and therefore can be applied to terahertz time domain spectroscopy and polarimetry. © 2006 Optical Society of America

OCIS codes: 260.5430, 260.3090, 230.5440, 260.1440.

The terahertz (THz) frequency range, located midway between microwaves and infrared light, presents a new frontier containing numerous technical applications and fundamental research problems. It has become a popular domain in spectroscopy and imaging, mostly using single-cycle electromagnetic pulses and time domain spectroscopy.[1] As a result of the increasing importance of this technique, much interest has been applied to characterizing the THz beams: divergence, spatial or frequency modes, and profiles. However, polarization has been much less studied. The key elements in polarimetry techniques are polarization converters and wave plates, but they usually depend on wavelength, and THz time domain spectroscopy has to deal with an ultrabroadband frequency range, sometimes exceeding a decade.[2] Then, THz achromatic wave plates are a prerequisite to designing precision polarimeters.

Standard birefringent wave plates made from birefringent materials can be used only at a single wavelength, since the retardation strongly depends on the wavelength.[3] Achromatic phase retarders can be designed on the basis of several techniques. Achromatic dephasing properties of total reflection can be used in Fresnel rhombs[3] or total reflection prisms,[4] but the systems are voluminous and often exhibit strong lateral shifts. Form birefringence of gratings[5,6] and liquid crystals[7] have also been used in the visible range; the combination of two wave plates of different materials can allow partial cancellation between the

dispersion of the two materials.[8] However, the resulting bandwidth is still too narrow for application in THz time domain spectroscopy.

In this Letter we show the design and experimental demonstration of a THz achromatic quartz (TAQ) quarter-wave plate that is insensitive to the wavelength for almost a decade. The design of the TAQ wave plate is based on the idea from Destriau and Prouteau.[9] Combining a standard half-wave plate and a standard quarter-wave plate, they succeeded in creating a new quarter-wave plate ($\pi/2$ dephasing), extending the bandwidth of the resulting retardation plate in the whole visible range. Later, this combination was applied to a variety of crystals and wavelengths.[10–12] The key feature is the partial cancellation of the change of retardation from each plate with respect to the frequency. To achieve the much larger bandwidth required to handle ultrashort THz pulses, we extended the design to a combination of up to six quartz plates. Quartz is reasonably transparent in the THz range,[2] with an amplitude absorption at 1 THz below 0.05 cm^{-1}. Quartz also exhibits strong birefringence: ordinary and extraordinary refractive indices are $n_o = 2.108$ and $n_e = 2.156$, respectively, at 1 THz. Amplitude absorption anisotropy $\alpha_o - \alpha_e$ remains below 0.02 cm^{-1} and has a negligible influence on retardation. The quartz plates are cut parallel to the optical axis and stacked together to form a unique wave plate. Each plate is described by its corresponding Jones matrix J_i ($i = 1-n$),[13]

$$J_i(\delta_i, \theta_i) = \begin{bmatrix} \cos \delta_i/2 + i \cos 2\theta_i \sin \delta_i/2 & i \sin 2\theta_i \sin \delta_i/2 \\ i \sin 2\theta_i \sin \delta_i/2 & \cos \delta_i/2 - i \cos 2\theta_i \sin \delta_i/2 \end{bmatrix},$$

which depends on two parameters: the dephasing $\delta_i = e_i(n_e - n_o)\nu/c$ and the orientation θ_i with respect to the optical axis. This leads to $2n$ independent parameters. The total Jones matrix is given by[14]

$$J = \prod_i J_i = \begin{pmatrix} A & B \\ -B^* & A^* \end{pmatrix},$$

Table 1. Calculated Thickness and Orientation of Quartz Plates 1–6

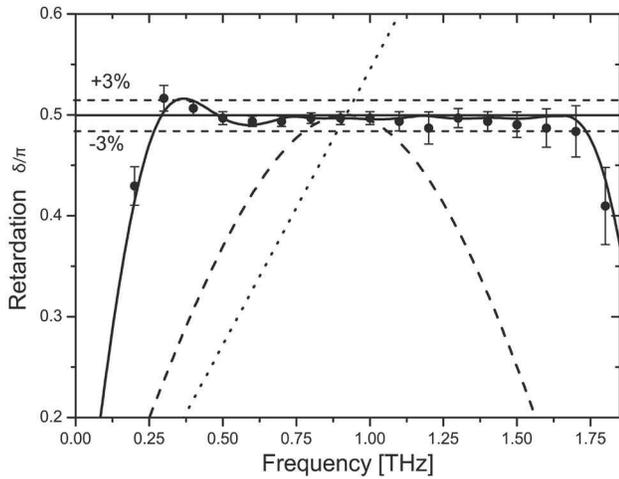|	1	2	3	4	5	6
Thickness (mm)	3.36	6.73	6.46	3.14	3.33	8.43
Angle (deg)	31.7	10.4	118.7	24.9	5.1	69.0

Fig. 1. Frequency dependence retardation of standard and TAQ quarter-wave plates. Relative bandwidth $\delta\nu/\nu$ is given at 3% bandwidth (horizontal lines). Comparison with a standard birefringent wave plate (dotted curve); two-plate combination (dashed curve) and the six-plate TAQ wave plate (solid curve, calculation; filled circles, data).

and the resulting retardation dephasing δ is obtained by

$$\tan^2\frac{\delta}{2} = \frac{|\mathrm{Im}\,A|^2 + |\mathrm{Im}\,B|^2}{|\mathrm{Re}\,A|^2 + |\mathrm{Re}\,B|^2}.$$

By use of a simulated annealing algorithm,[15] the parameters of the n quartz plates have been optimized to minimize the error function $\Sigma_\nu[\delta(\nu) - \pi/2]^2$ over the frequency range of 0.2–2 THz, including the frequency dependence of the refractive indices. We performed simulations for any combination of up to seven plates. As expected, the available bandwidth is extended with the number of plates. Our experimental THz range was already covered by a combination of six plates, which is a good compromise between the available bandwidth and the total thickness of the achromatic wave plate. The calculated thickness and orientation for the six quartz plates are given in Table 1. The result obtained with the combination of the six plates, depicted in Fig. 1 (solid curve), shows remarkably large retardation stability over the whole THz range. The bandwidth at 3% from ideal $\pi/2$ dephasing extends from 0.25 to 1.75 THz. The total thickness of the TAQ wave plate is 31.4 mm, corresponding to an amplitude transmission at 1 THz measured to be equal to 74%. Each plate is designed with a thickness precision of better than 10 μm, and the relative angular adjustment between the plates is better than 1° to maintain the high quality of the wave plate. The 30 mm diameter plates are stacked together at visible optical contact without any cement, and in this case no reflection occurs at the in-
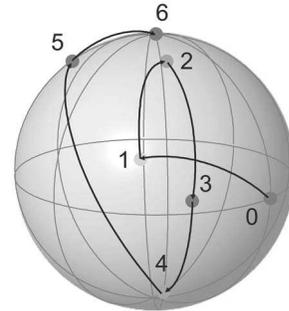

Fig. 2. Poincaré sphere representation of polarization state evolution through the six quartz plates of the TAQ wave plate. When the incident polarization (0) is linear, the polarization output of the TAQ wave plate (6) is circular.

terface between the plates. Angular acceptance of the retarder has been found to be ±1.5° at a 3% change of dephasing, which is typical for plate retarders.[12] Representation of the evolution of the polarization state through the quartz plates is done by a Poincaré sphere.[3] Figure 2 shows the case of a linearly polarized incident wave (0) that undergoes six polarization state transitions ($1\rightarrow5$) before exiting as a circularly polarized light (6). When frequency varies, the dephasing of each individual plate changes. The corresponding points (1)–(5) on the Poincaré sphere then move, but the final polarization state (6) remains perfectly circular, as expected from an achromatic quarter-wave plate.

To measure the retardation of the TAQ wave plate in the THz range, we developed a new technique of ellipsometry by using rotating linear polarizers. This technique allows a precise determination of the retardation and orientation of the wave plate without moving the detecting antenna. In our experiment [see Fig. 3(A)], we generate and coherently detect broadband polarized single-cycle pulses of THz radiation by illuminating photoconductive antennas with two synchronized 80 fs laser pulses.[16] The incident THz beam is modulated by a chopper, and a lock-in amplifier detects the current induced by the transmitted THz radiation in the detector. A delay line allows us to scan the amplitude of the electric field. The TAQ wave plate and the two polarizers used for polarimetry are positioned between two steering paraboloid mirrors that produce a parallel 15 mm waist frequency-independent THz beam. A linearly polarized electric field E_0 is sent through the wave plate to be investigated. The exiting electric field E carries out information on the wave plate as

$$\underline{E} = a\,\cos(\omega t)\mathbf{x} + b\,\cos(\omega t + \delta)\mathbf{y}, \tag{1}$$

where a, b, and δ, the ellipticity parameters, directly refer to the retardation and orientation of the wave
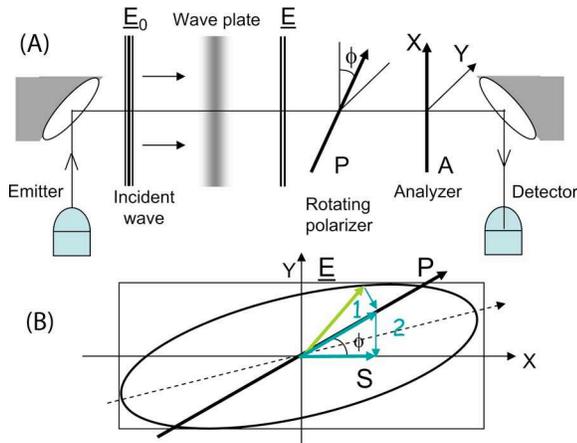
Fig. 3. (Color online) (A) Setup for polarimetry measurements of the wave plate. (B) Projection of the electric field E on the rotating polarizer and fixed analyzer gives the measured signal $S(\phi)$.
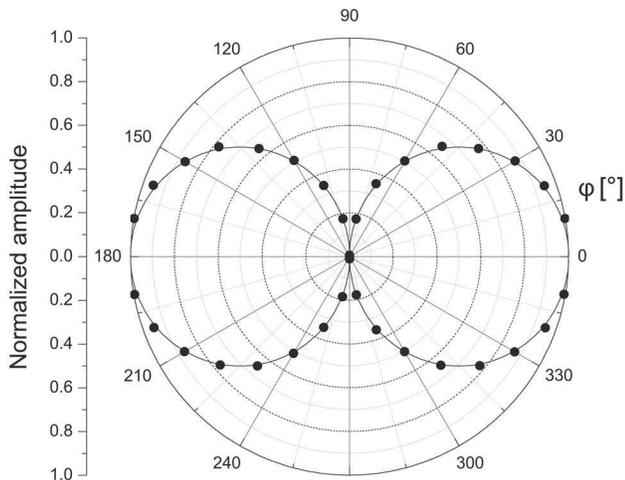

Fig. 4. Normalized amplitude of the signal from polarimetry measurements versus the angle ϕ of the fixed polarizer in polar coordinates. The spectral component is at 1 THz. Filled circles, data; solid curve, theoretical fit.

plate. Then two linear THz polarizers are used [Fig. 3(A)]. The first polarizer, oriented at an angle ϕ with respect to $\mathbf{x}$, is followed by a fixed polarizer along $\mathbf{x}$, called the analyzer. Considering the general case of the incident wave exiting from the wave plate, the two polarizers perform two successive projections of the electric field, along the polarizer and analyzer directions, ϕ and $\mathbf{x}$, respectively [see Fig. 3(B)]. One easily obtains the amplitude $S(\phi)$ of the resulting electric field:

$$S(\phi) = \cos\phi[(a\cos\phi + b\sin\phi\cos\delta)^2$$
$$+ (b\sin\phi\sin\delta)^2]^{1/2}. \qquad (2)$$

The ellipticity parameters are obtained by recording S versus the angle of the polarizer ϕ. Spatial cases of linear (along $\mathbf{x}$) and circular waves give $S(\phi) = a\cos^2(\phi)$ and $S(\phi) = a\cos\phi$, respectively. In our

experiment the signal has been recorded in steps of 10° of the polarizer angle ϕ, leading to 36 scans. Then, spectral data have been achieved by Fourier transform of the temporal scans. A typical result is presented in Fig. 4. The data (solid circles) are in excellent agreement with the theoretical fit from Eq. (2) (solid curves), with a dephasing of $\pi/2$. The total dephasing is then extracted for each frequency. Experimental dephasing of the six-plate quartz TAQ wave plate is depicted in Fig. 1 (solid circles) from 0.2 to 1.8 THz. Agreement with the theoretical curve from the Jones matrices calculation is very good. Note the increase of the measurement uncertainty at both ends of the spectrum as a result of the drop of the reference signal. The 3% bandwidth of the TAQ wave plate extends from 0.25 to 1.75 THz, centered around 0.92 THz, representing a factor $\nu_{max}/\nu_{min} = 7$ in frequency expansion. In relative bandwidth $\delta\nu/\nu$, this wave plate covers more than 160%, which is 25 times bigger than for a standard quarter-wave plate.

In conclusion, we have designed and characterized by polarimetry a terahertz achromatic quartz quarter-wave plate. The TAQ wave plate, made from six quartz plates precisely adjusted and stacked together, exhibits a huge bandwidth that covers the entire spectrum required for THz time domain spectroscopy.

References

1. D. Mittleman, *Sensing with Terahertz Radiation*, Springer Series in Optical Sciences (Springer, 2003).
2. D. Grischkowsky, S. R. Keiding, M. van Exter, and C. Fattinger, J. Opt. Soc. Am. B **7**, 2006 (1990).
3. M. Born and E. Wolf, *Principles of Optics*, 6th ed. (Cambridge University Press, 1997).
4. R. M. A. Azzam and C. L. Spinu, J. Opt. Soc. Am. A **21**, 2019 (2004).
5. N. Bokor, R. Shechter, N. Davidson, A. A. Friesem, and E. Hasman, Appl. Opt. **40**, 2076 (2001).
6. G. P. Nordin and P. C. Deguzman, Opt. Express **5**, 163 (1999).
7. S. Shen, J. She, and T. Tao, J. Opt. Soc. Am. A **22**, 961 (2005).
8. J. M. Beckers, Appl. Opt. **10**, 973 (1971).
9. G. Destriau and J. Prouteau, J. Phys. Radium **8**, 53 (1949).
10. P. Hariharan, Opt. Eng. **35**, 3335 (1996).
11. B. Boulbry, B. Bousquet, B. L. Jeune, Y. Guern, and J. Lotrian, Opt. Express **9**, 225 (2001).
12. J. M. Beckers, Appl. Opt. **11**, 681 (1972).
13. R. C. Jones, J. Opt. Soc. Am. **31**, 488 (1941).
14. H. Hurwitz and R. C. Jones, J. Opt. Soc. Am. **31**, 493 (1941).
15. W. H. Press, S. A. Teukolsky, W. T. Vetterling, and B. P. Flannery, *Numerical Recipes in C* (Cambridge U. Press, 1992).
16. C. Fattinger and D. Grischkowsky, Appl. Phys. Lett. **54**, 490 (1989).